



HAL
open science

Shift contagion and minimum causal intensity portfolio during the COVID-19 and the ongoing Russia-Ukraine conflict

Mondher Bouattour, Amine Ben Amar, Stéphane Goutte, Makram Bellalah

► **To cite this version:**

Mondher Bouattour, Amine Ben Amar, Stéphane Goutte, Makram Bellalah. Shift contagion and minimum causal intensity portfolio during the COVID-19 and the ongoing Russia-Ukraine conflict. 2023. halshs-04064084

HAL Id: halshs-04064084

<https://shs.hal.science/halshs-04064084>

Preprint submitted on 10 Apr 2023

HAL is a multi-disciplinary open access archive for the deposit and dissemination of scientific research documents, whether they are published or not. The documents may come from teaching and research institutions in France or abroad, or from public or private research centers.

L'archive ouverte pluridisciplinaire **HAL**, est destinée au dépôt et à la diffusion de documents scientifiques de niveau recherche, publiés ou non, émanant des établissements d'enseignement et de recherche français ou étrangers, des laboratoires publics ou privés.

Shift contagion and minimum causal intensity portfolio during the COVID-19 and the ongoing Russia-Ukraine conflict

Authors

Amine Ben Amar^{a,b}, Mondher Bouattour^a, Makram Bellalah^b & Stéphane Goutte^c

^a *Dept. of Finance, Excecia Business School, 17024, La Rochelle, France.*

^b *Laboratoire d'Economie, Finance, Management & Innovation - LEFMI [UR 4286], University of Picardie Jules Verne, Amiens, France.*

^c *UMI SOURCE, Paris-Saclay University, Paris, France.*

Abstract

Using the TYDL causality test, this paper attempts (i) to investigate the existence of *shift contagion* among a large spectrum of financial markets during recent stress and stress-free periods and (ii) to propose a new approach of portfolio management based on the minimization of the causal intensity. During the COVID-19 crisis period, the *shift contagion* analysis not only reveal a tripling of the causal links between the markets studied, but also a change in the causal structure. Beyond the initial impact of the COVID-19 crisis on financial markets, policy interventions seem to have helped in reassuring market participants that the further spread of financial stress would be mitigated. However, the Russian-Ukrainian, and the high degree of uncertainty it entailed, has again exacerbated the interdependencies between financial markets. In terms of portfolio analysis, our minimum-causal-intensity approach records a lower (respectively higher) reward-to-volatility ratio than the Markowitz (1952 & 1959) minimum-variance traditional approach during the pre-COVID-19 (respectively pre-war) period. On the other hand, both approaches, the one we propose in this paper and the minimum-variance approach, record negative reward-to-volatility ratios during crisis periods.

Keywords: Shift contagion, diversification, minimum-causal intensity portfolio, clean energy, financial market, cryptocurrencies, socially responsible investment.

1. Introduction

Since the 1980s, many factors, such as financial deregulation, the development of new information technologies, as well as financial innovations, have further increased the interdependence among financial markets (Gamba-Santamaria et al., 2019), which implies greater interactions and interdependencies between the different segments of the financial markets. Obviously, more integrated financial markets provide investors with a wider range of investment opportunities, enhance the possibility of risk sharing and thus lead to more efficient portfolio management. Nevertheless, a high level of integration can weaken the resilience of the financial system, as it results in faster transmission of shocks among markets, amplifies their effects, and thereby exacerbates systemic risk. History provides us with evidence. Throughout the past three decades, financial crises have not only propagated across markets and economies more rapidly than in the past, but have also been more protracted and disruptive (Forbes and Rigobon, 2002; Aït-Sahalia et al., 2015; Awartani et al., 2016; Bala & Takimoto, 2017; Mieg, 2020; Zhang & Broadstock, 2020), deeply impacting social welfare (Kwon and Holliday, 2006; Schwartz, 2012). The crisis resulting from the COVID-19 pandemic is a recent example. Indeed, several studies have shown that this health crisis suddenly amplified the interdependence between financial markets, causing a simultaneous fall of the major financial markets by the end of February 2021 (Kohlscheen et al., 2020; Zhang et al. 2020). As a result, academics, policymakers, and investors have once again focused on analysing the connectedness, as well as shift contagion between financial markets during this crisis (among others: Corbet et al. 2020; Broadstock et al. 2021; Corbet et al. 2021; Bélaïd et al. 2021; Ben Amar et al. 2021; Yarovaya et al. 2022; Uddin et al. 2022; Corbet et al. 2022).

Understanding the connectedness as well as shift contagion among different financial markets during stress and stress-free periods would provide decision makers, regulators and investors, with very useful information (Kang et al., 2016). Regulators need to understand the extent of interdependencies among financial markets in order to promote the stability and resilience of the financial system (Karolyi, 1995; Caporale et al., 2002; Lee et al., 2015, Liu et al., 2019). For investors, a better understanding of the interdependence between financial markets would allow for more effective diversification and hedging strategies (King and Wadhvani, 1990; Silvennoinen and Thorp, 2013).

The literature has paid considerable attention to the study of connectedness and shift contagion among financial markets. Indeed, a sizable body of literature has examined in depth the connectedness and shift contagion between stock markets (Marais and Bates, 2006; Diebold & Yilmaz, 2009; Belke and Dubova, 2018; Ben Amar et al., 2020), commodity markets (Chang et al., 2011; Pan et al., 2014), commodity and non-commodity markets (Arouri et al., 2011; Basher and Sadorsky, 2016; Barbaglia et al., 2020; Asl et al., 2021), stock markets and cryptocurrencies (Jeribi and Masmoudi, 2021; Ghorbel et al., 20022), green bonds, renewable energy stocks and carbon markets (Tiwari et al., 2022) and clean energy and technology indices (Niu, 2022; Hemrit and Benlagha, 2022). However, the way investors can use the results of this strand of the literature in their portfolio diversification strategies remains largely unexplored.

This paper contributes to the existing literature by proposing a new approach to portfolio diversification based on minimizing the causal intensity between markets. Indeed, the goal of this study is three-fold. First, using the TYDL causality test, it investigates the structure of causal links between different segments of the financial market (commodities, stocks, socially

responsible investments, sovereign bonds, green bonds, cryptocurrencies and clean energies) during recent stress and stress-free periods. Relatively to previous works, our study covers a high representative number of financial markets including commodities, stocks, bonds and cryptocurrencies. Investigating the causal structure between these different markets will help to understand the extent to which markets are segmented or interconnected during both stress and stress-free periods, allowing investors to better structure their portfolios and manage risk. In our study, two stress periods are included to the analysis: the COVID-19 crisis and the ongoing Russia-Ukraine war. Second, it uses a measure of causal intensity to examine the existence of *shift contagion*¹ during stress periods, *i.e.* significant changes in causal links among the considered markets before and during the stress periods. Finally, it proposes a new approach of portfolio management minimizing the causal intensity among the underlying assets. Indeed, by using the Toda and Yamamoto (1995) and Dolado and Lütkepohl (1996) causality test, we extend the traditional minimum-variance portfolio framework of Markowitz (1952 & 1959) and propose a new minimum causality approach.

The results of this paper are of practical interest to investors. Indeed, beyond a better understanding of the interdependence structure between the different financial markets, this study proposes to take this interdependence structure into account in portfolio management in order to cope with systemic risk.

The remainder of this paper is organized as follows: Section 2 describes the data and outlines the empirical strategy. Section 3 documents and discuss the empirical results. Section 4 concludes the paper.

2. Methods and materials

The present study focuses on evaluating *shift contagion* during recent stress periods (the COVID-19 crisis period and the ongoing Russia-Ukraine war period), as well as portfolio management. The study was conducted for selected assets – commodities, stocks, socially responsible investments, sovereign bonds, green bonds, cryptocurrencies, and clean energies – covering a large spectrum of financial markets' segments. The analysis of causal structures during stress and stress-free was carried out for these selected assets to (i) capture shift contagion and (ii) to construct a portfolio minimizing the causal intensity among the underlying assets. Subsection 2.1 describes the data used and the periods examined, and subsection 2.2 outlines the methodology.

2.1. Data

Our underlying datasets are daily observations of broad spectrum of assets: a global stock market index, a global sovereign bonds index, a global green bonds index, a global information technology index, a socially responsible investment index, two clean-energy related indexes, a cryptocurrency, and two representative commodity price indexes (See Table 1).

¹ Marais and Bates (2006) define *shift contagion* as “significant differences in cross-market links between tranquil and crisis periods”. It should be noted that the *shift contagion* concept was first indicated in a study by Forbes and Rigobon (2000) to describe the increase in co-movements among markets after a shock.

Table 1. List of Indices

Indices		Description
MSCI ACWI Index	ACWI	The MSCI ACWI Index is a representative global stock market index. It covers approximately 85% of the global stock market capitalization.
S&P Global Developed Sovereign Bond Index	SBND	The S&P Global Developed Sovereign Bond Index tracks the performance of sovereign bonds issued by developed countries.
S&P Green Bond Index	GRNB	The S&P Green Bond Index tracks the performance of bonds whose proceeds are used to finance environmentally friendly projects
MSCI ACWI Information Technology Index	IT	The MSCI ACWI IT Index is representative of the performance of global Information Technology companies.
MSCI KLD 400 Social Index	KLD	The MSCI KLD 400 Social Index consists of 400 US securities providing exposure to companies having high ESG ratings relative to the constituents in the MSCI US Investable Market.
Wilderhill Clean Energy Index	CLN	The Wilderhill Clean Energy Index tracks the performance of businesses engaged in the clean energy activities.
Wilderhill New Energy Global Innovation Index	INV	The Wilderhill New Energy Global Innovation Index tracks the performance of worldwide businesses whose innovative technologies and services focus on generation and use of cleaner energy, conservation, efficiency and advancing renewable energy.
Bitcoin	BTCN	The Bitcoin is a digital currency that operates on the blockchain. It is not only the first cryptocurrency, but also the largest in terms of capitalization.
S&P GSCI Energy Spot Index	NRG	The S&P GSCI Energy Spot Index provides investors with a reliable benchmark of the investment performance in the energy commodity sector.
S&P GSCI Non-Energy Spot Index	NNRG	The S&P GSCI Non-Energy Spot Index provides investors with a reliable aggregated benchmark of the investment performance in the non-energy markets.

All series, expressed in U.S. dollars, are collected from Refinitiv Eikon Datastream and cover the period running from January 2nd, 2019 to November 7th, 2022. This period is informative in terms of market development because it covers both calm periods and periods of turbulence during which shocks may spread between markets at different intensities. To investigate the existence of *shift contagion* during stress periods, the causality is tested distinguishing the tranquil pre-COVID-19 period (from January 2nd, 2019 to December 31st, 2019), the COVID-19 crisis period (from January 1st, 2020 to March 31st, 2020), the pre-war period (from April 1st, 2020 to February 23rd, 2022), and the Russia-Ukraine war period (from February 24th, 2022 to November 7th, 2022). The separation between the pre-COVID-19 and the COVID-19 periods can be justified by the beginning of availability of data on COVID-19, as the first case was reported to the World Health Organization Country Office in China on December 31, 2019. To assess the initial impact of the COVID-19 medical shock on financial markets, we limit the COVID-19 period to the first quarter of the year 2020 (2020Q1). Indeed, the collapse of almost all financial markets around the world during 2020Q1 provide a snapshot of how market participants process information as disaster strikes. From the second quarter of the year 2020 (2020Q2), the markets reacted to the different economic policies that were implemented to avoid the collapse of the financial system, which is why we consider the period between April 1st, 2020, and February 23rd, 2022 as a stress-free period. February 24th, 2022 marks the beginning of the war between Ukraine and Russia. Thus, we also examine the impact of the ongoing war on the causal structure between the markets considered.

2.2. Empirical strategy

Our empirical strategy consists of two complementary steps. First, we use the TYDL causality test to investigate *shift contagion* and compute the causal structure among the markets considered. Second, we use the results of the first step to construct a portfolio minimizing the causal intensity among the underlying assets.

2.2.i. TYDL Causality test

In this study we use the TYDL causality test, based on the works of Toda and Yamamoto (1995) and Dolado and Lütkepohl (1996), to (i) investigate possible *shift contagion*, *i.e.* significant changes in the number and magnitudes of causal linkages between a set of financial markets during stress and stress-free periods (Marais and Bates, 2006, Ben Amar et al. 2021; Bélaïd et al. 2021)² and (ii) compute the causal intensities matrix.

The TYDL causality test is reliable whatever the variables' order of integration, *i.e.* that time-series could be $\mathbf{I}(0)$, $\mathbf{I}(1)$ or $\mathbf{I}(2)$, which is consistent with financial time-series. The TYDL causality test involves two steps. The first step consists in identifying the order \mathbf{p} of the vector autoregressive (VAR) model on which the causal analysis will be conducted. This autoregressive order \mathbf{p} is nothing but the sum of the optimal autoregressive order \mathbf{k} of the VAR model and the maximum integration order \mathbf{I}_{\max} of the endogenous variables within the VAR model, *i.e.*, $\mathbf{p} = \mathbf{k} + \mathbf{I}_{\max}$. Indeed, the inclusion of the additional \mathbf{I}_{\max} lags in the level-estimated VAR model is required as it allows considering the potentially cointegrated characteristic of time series. Through the estimation of $\text{VAR}(\mathbf{p})$, there is a guarantee in the asymptotic χ^2 distribution of the Wald statistic (Marais and Bates, 2006).

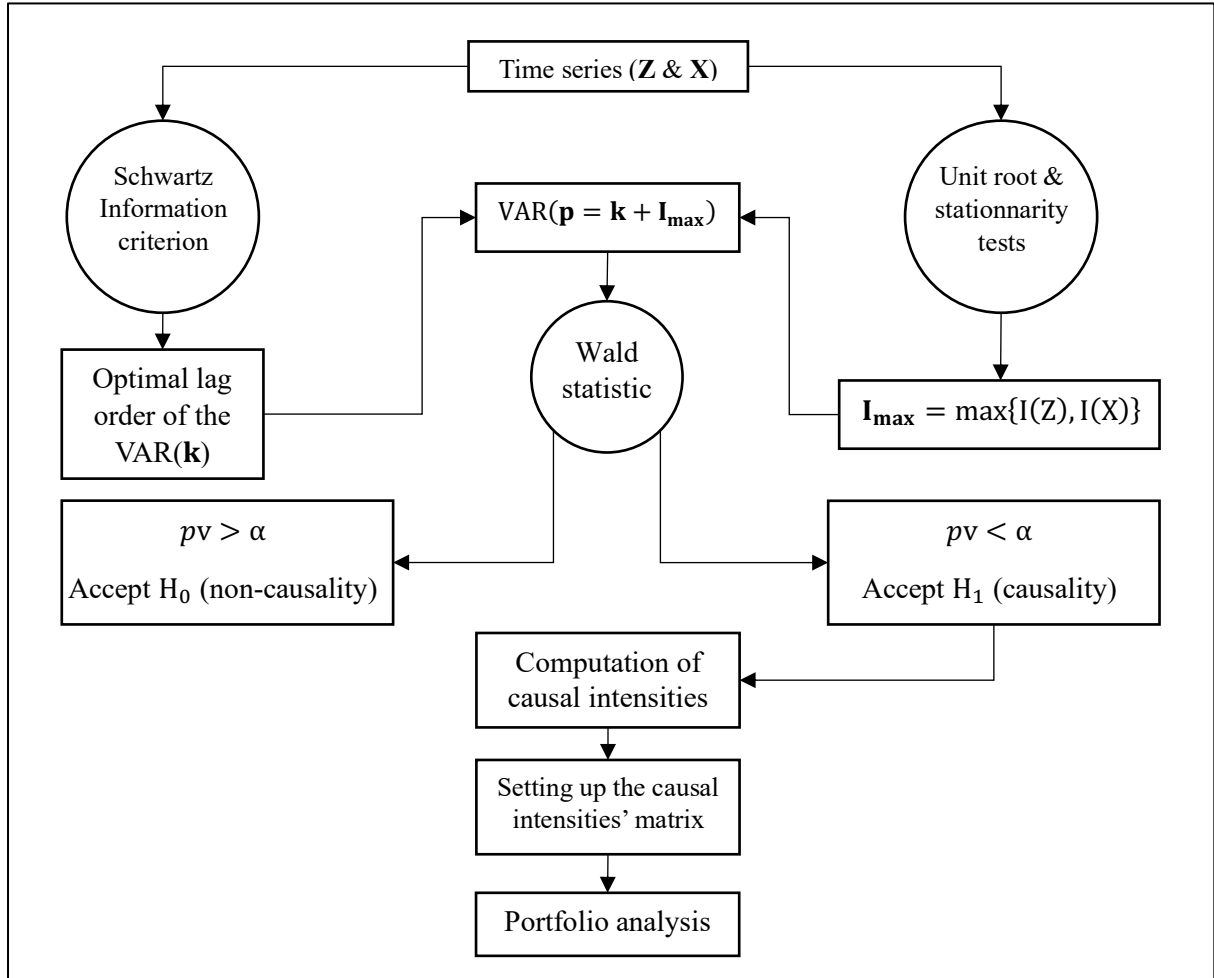
Given the small period of observation during crisis and war periods, \mathbf{k} must be obtained from an information criterion that does not over-parametrize the VAR system in order to minimize the loss of power of the TYDL causality test (Saikkonen and Lütkepohl, 1996). Thus, the Schwartz (1978) Information Criterion is employed to identify \mathbf{k} , and the Phillips and Perron (1988) unit root test and the Kwiatkowski, Phillips, Schmidt, and Shin (1992) stationarity test are used to determine \mathbf{I}_{\max} . Therefore, the $\text{VAR}(\mathbf{p})$, estimated by ordinary least squares, describes well the joint dynamics of the endogenous variables, independently of their integration order.

The second step is to test the null hypothesis (H_0) of non-causality against the alternative hypothesis (H_1) of Granger causality using standard Wald statistic that takes into account only the first \mathbf{k} coefficients matrices³. The alternative hypothesis H_1 is accepted (*i.e.*, causality) when the p -value of the Wald statistic is lower than the significance level α . Otherwise, the non-causality hypothesis (H_0) is accepted. It should be noted that the two steps on which the TYDL causality test is performed are applicable only if $\mathbf{I}_{\max} \leq \mathbf{k}$ (Toda and Yamamoto, 1995).

² According to Marais and Bates (2006), *shift contagion* can be defined as “significant differences in cross-market links between tranquil and crisis periods”. The *shift contagion* concept was first appeared in a study by Forbes and Rigobon (2000) to describe the increase in co-movements among markets after a shock.

³ For further details about the Wald test, we refer the interested readers to Dolado and Lütkepohl (1996).

Fig.1 Empirical strategy: TYDL causality test steps & portfolio analysis



Note: pv represents the marginal significance level associated with the null hypothesis H_0 of non-causality.

Once H_0 rejected, and since the data is expressed in logarithms, Marais and Bates (2006) suggest to derive the elasticity e_{ZX} of the caused variable Z with respect to the causal variable X based on the estimated coefficients of the VAR(p) and use it as a measure of the magnitude of the causal relation. For instance, let $(Z_t, X_t)'$ the 2×1 dimensional vector of endogenous variables. The VAR(p) model is expressed as follows:

$$\begin{cases} Z_t = \sum_{i=1}^k \gamma_{1i} Z_{t-i} + \sum_{j=k+1}^p \gamma_{1j} Z_{t-j} + \sum_{i=1}^k \beta_{1i} X_{t-i} + \sum_{j=k+1}^p \beta_{1j} X_{t-j} + \varepsilon_{Zt} \\ X_t = \sum_{i=1}^k \gamma_{2i} Z_{t-i} + \sum_{j=k+1}^p \gamma_{2j} Z_{t-j} + \sum_{i=1}^k \beta_{2i} X_{t-i} + \sum_{j=k+1}^p \beta_{2j} X_{t-j} + \varepsilon_{Xt} \end{cases}$$

2.2.ii. Minimum-causal intensity portfolio

After the causality from the variable \mathbf{X} to the variable \mathbf{Z} is confirmed from the TYDL test, $\mathbf{e}_{\mathbf{ZX}}$ is derived from the first equation of the VAR system as follows:⁴

$$\mathbf{e}_{\mathbf{ZX}} = \frac{\sum_{i=1}^k \beta_{1i} + \sum_{j=k+1}^p \beta_{1j}}{1 - \sum_{i=1}^k \gamma_{1i} - \sum_{j=k+1}^p \gamma_{1j}}$$

and $\mathbf{e}_{\mathbf{XZ}}$ is derived from the second equation of the system as follows:

$$\mathbf{e}_{\mathbf{XZ}} = \frac{\sum_{i=1}^k \gamma_{2i} + \sum_{j=k+1}^p \gamma_{2j}}{1 - \sum_{i=1}^k \beta_{2i} - \sum_{j=k+1}^p \beta_{2j}}$$

These elasticities reflect the magnitude of the causal relationship between the two variables in the system: the greater the elasticities, the stronger the causal relationship between \mathbf{X} and \mathbf{Z} . Thus, the causal intensities matrix is given by:

$$\Phi_{\mathbf{ZX}} = \begin{pmatrix} \mathbf{e}_{\mathbf{XX}} & \mathbf{e}_{\mathbf{XZ}} \\ \mathbf{e}_{\mathbf{ZX}} & \mathbf{e}_{\mathbf{ZZ}} \end{pmatrix} = \begin{pmatrix} 1 & \mathbf{e}_{\mathbf{XZ}} \\ \mathbf{e}_{\mathbf{ZX}} & 1 \end{pmatrix}$$

with

$$\mathbf{e}_{\mathbf{ZX}} = \begin{cases} \frac{\sum_{i=1}^k \beta_{1i} + \sum_{j=k+1}^p \beta_{1j}}{1 - \sum_{i=1}^k \gamma_{1i} - \sum_{j=k+1}^p \gamma_{1j}} & \text{if } H_1 \text{ is accepted} \\ \mathbf{0} & \text{if } H_0 \text{ is accepted} \end{cases}$$

and

$$\mathbf{e}_{\mathbf{XZ}} = \begin{cases} \frac{\sum_{i=1}^k \gamma_{2i} + \sum_{j=k+1}^p \gamma_{2j}}{1 - \sum_{i=1}^k \beta_{2i} - \sum_{j=k+1}^p \beta_{2j}} & \text{if } H_1 \text{ is accepted} \\ \mathbf{0} & \text{if } H_0 \text{ is accepted} \end{cases}$$

Based on $\mathbf{e}_{\mathbf{ZX}}$ and $\mathbf{e}_{\mathbf{XZ}}$, we can calculate the pairwise elasticity, $\bar{\mathbf{e}}$, measuring the overall inter-elasticity between the two variables \mathbf{X} and \mathbf{Z} as:

$$\bar{\mathbf{e}} = \frac{1}{2} (\mathbf{e}_{\mathbf{ZX}} + \mathbf{e}_{\mathbf{XZ}})$$

This metric illustrates the average magnitude of bilateral causal elasticity across variables \mathbf{X} and \mathbf{Z} , and allows us to extract the following symmetric causal intensities matrix:

$$\bar{\Phi} = \begin{pmatrix} 1 & \frac{\mathbf{e}_{\mathbf{XZ}} + \mathbf{e}_{\mathbf{ZX}}}{2} \\ \frac{\mathbf{e}_{\mathbf{ZX}} + \mathbf{e}_{\mathbf{XZ}}}{2} & 1 \end{pmatrix}$$

If we examine the causal structure for N variables, the causal intensities matrix, $\bar{\Phi}_N$, becomes:

⁴ To investigate the existence of shift contagion among the markets considered, and to be able to compute the price-elasticity linkages between them as well as the causal-intensities matrix, a log-transformation of the data is chosen, as in Marais and Bates (2006). Descriptive statistics may be provided from the authors upon request.

$$\bar{\Phi}_N = \begin{pmatrix} 1 & \frac{\mathbf{e}_{1,2} + \mathbf{e}_{2,1}}{2} & \dots & \frac{\mathbf{e}_{1,N-1} + \mathbf{e}_{N-1,1}}{2} & \frac{\mathbf{e}_{1,N} + \mathbf{e}_{N,1}}{2} \\ \frac{\mathbf{e}_{2,1} + \mathbf{e}_{1,2}}{2} & 1 & \dots & \frac{\mathbf{e}_{2,N-1} + \mathbf{e}_{N-1,2}}{2} & \frac{\mathbf{e}_{2,N} + \mathbf{e}_{N,2}}{2} \\ \vdots & \vdots & \ddots & \vdots & \vdots \\ \frac{\mathbf{e}_{N-1,1} + \mathbf{e}_{1,N-1}}{2} & \frac{\mathbf{e}_{N-1,2} + \mathbf{e}_{2,N-1}}{2} & \dots & 1 & \frac{\mathbf{e}_{N-1,N} + \mathbf{e}_{N,N-1}}{2} \\ \frac{\mathbf{e}_{N,1} + \mathbf{e}_{1,N}}{2} & \frac{\mathbf{e}_{N,2} + \mathbf{e}_{2,N}}{2} & \dots & \frac{\mathbf{e}_{N,N-1} + \mathbf{e}_{N-1,N}}{2} & 1 \end{pmatrix}$$

Once we have obtained the causal intensities matrix, we explore historical investment performance by back-testing portfolios. Thus, we build on and extend the Markowitz (1952 & 1959) framework and propose to use the causal-intensities matrix to derive the vector of portfolio weights. According to the minimum-causal-intensities (MIN-CAI) approach, the vector of weights, $\omega^{\text{MIN-CAI}} = (\omega_1^{\text{MIN-CAI}}, \dots, \omega_N^{\text{MIN-CAI}})'$, is given by

$$\omega^{\text{mc}} = \frac{\bar{\Phi}_N^{-1} \mathbf{1}}{\mathbf{1}' \bar{\Phi}_N^{-1} \mathbf{1}}$$

where $\omega^{\text{MIN-CAI}}$ is a $N \times 1$ dimensional vector of weights, such as the sum of these weights equals one.⁵ $\mathbf{1}$ is a $N \times 1$ dimensional vector with each element equal one, and $\bar{\Phi}$ is the $N \times N$ dimensional causal-intensities matrix. Indeed, the merit of this approach, comparatively to the Markowitz (1952 & 1959) minimum-variance traditional approach, is that it allows the construction of portfolios that reduce the causal intensities between the underlying assets and, consequently, makes portfolios more resilient to systemic risk.

3. Results

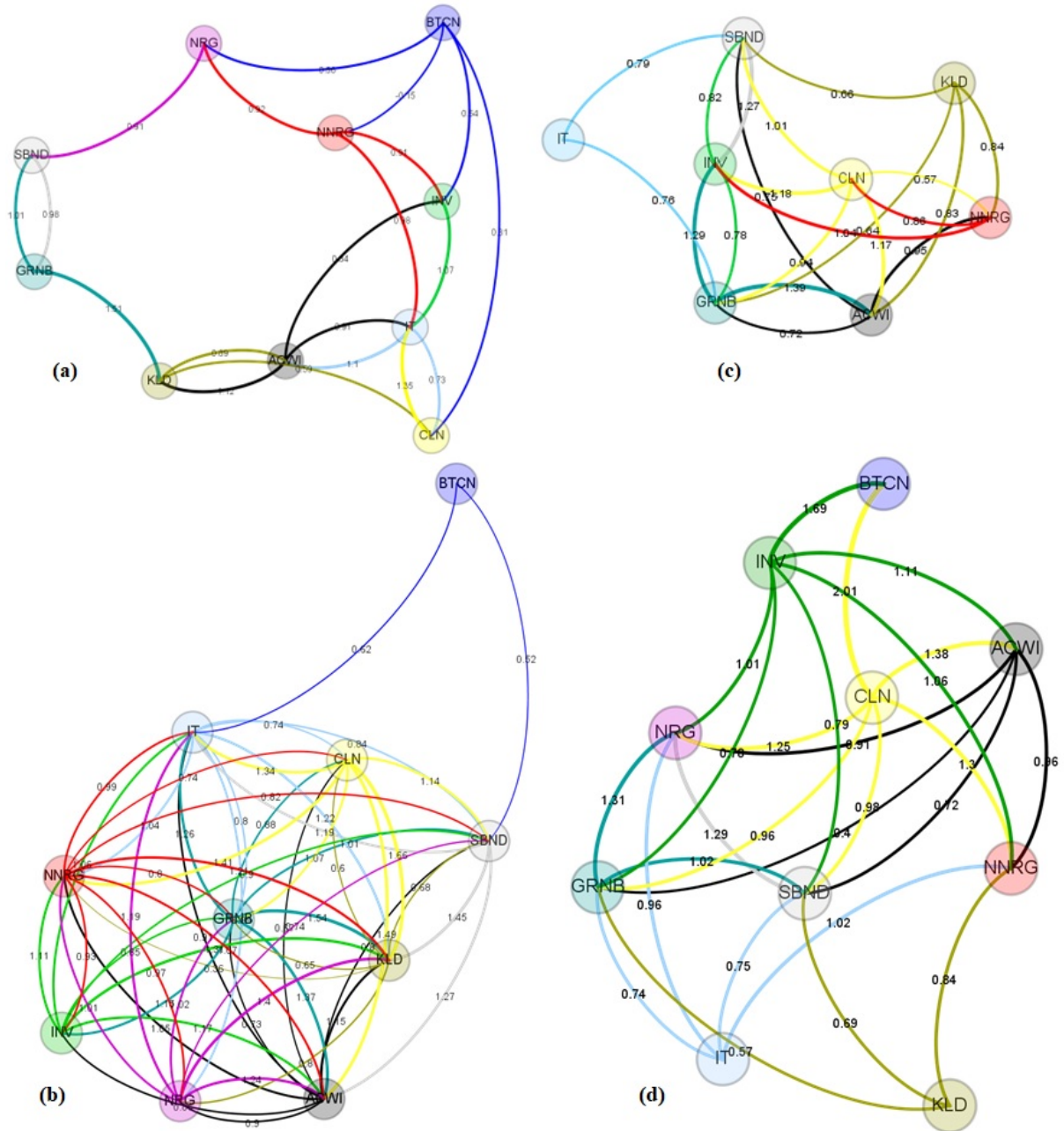
3.1. Shift contagion analysis

Selected descriptive statistics of the log daily data are summarized in Table 2 in the appendices. The order of integration of the time-series used is almost equal to one (See Table 2 in the appendices)⁶. The results of the TYDL causality test and the measure of causal intensities are detailed in Tables 3 to 6 in the appendices and summed up by Figures 2.a, 2.b, 2.c and 2.d.

⁵ Weights may be negative, which refers to short sale.

⁶ The Phillips-Perron unit-root test (Phillips and Perron, 1988) and the KPSS stationarity test (Kwiatkowski et al., 1992) are not reported in this paper, but they are available from the authors upon request.

Fig.2 Causal links during stress and stress-free periods

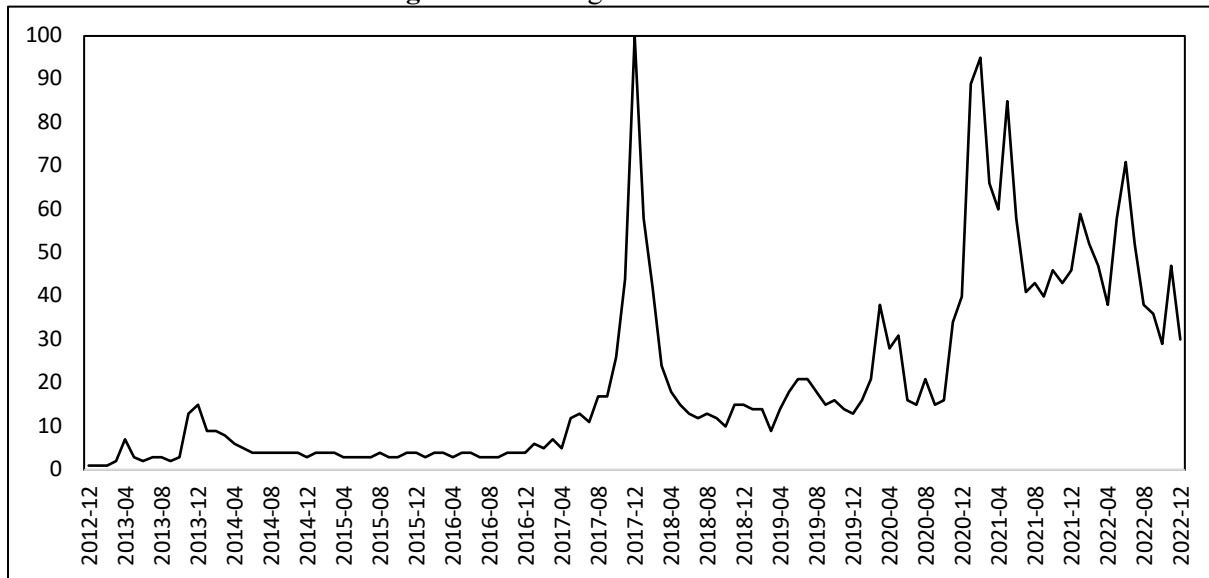


Note: (a) pre-COVID-19 period; (b) COVID-19 period; (c) pre-war period; (d) Russia-Ukraine war period. See Table 1 for abbreviations. The ForceAtlas2 algorithm of Jacomy et al. (2014) is used to determine the locations of nodes.

During the pre-COVID-19 tranquil period, BTCN appears to have a major influence on the rest of the market considered. Indeed, the causal structure depicted in Figure 2.a shows that it influences NRG, NNRG, INV and CLN markets. Indeed, interest in crypto-currencies in general, and bitcoin in particular, as an investment asset class began in late 2016, as evidenced by the steady (albeit slow) price increases throughout that year and into 2017, when the price of bitcoin broke the \$1,000 mark. There was massive media coverage of this phenomenon, which further piqued investor interest and, in turn, put upward pressure on prices throughout the year to break the \$19,000 mark. It is worth noting that even the intensity of bitcoin searches in Google increased significantly from the end of 2016, and peaked towards the end of 2017 (see Fig.3). The growing awareness of investors since 2017 seems to strengthen the correlation

between crypto-currency prices and those in other financial markets, which is consistent with our results during the pre-COVID-19 stress-free period. The COVID-19 pandemic created and exacerbated concerns in the financial markets due to the sudden slowdown in global economic activity. Many investors withdrew from the stock market and placed their money into Bitcoin during the COVID-19 crisis period, whose price more than quadrupled between the first quarter of 2020 and the first quarter of 2021. This potentially explains the decline in correlation between Bitcoin and other financial markets and, in turn, the decline in the influence of BTCN during the COVID-19 crisis period (see Fig.2.b).

Fig.3 Global Google Search on Bitcoin



Source: <https://trends.google.com> (download on December 12, 2022)

Moreover, the results of the TYDL causality test (See Tables 3 to 6 and Figures 2.a to 2.d) show that all the elasticities are positive (*i.e.* $e_{zx} > 0$) and suggest an increase in the number of causal links between the stress-free and stress periods. Indeed, relatively to the pre-COVID-19 stress-free period, the COVID-19 crisis period (*i.e.* Q1 2020) is characterized by the presence of many linkages among the markets considered. Specifically, we identify 20 causal relationships during the pre-COVID-19 period and 56 during the COVID-19 crisis period (about 30% of which emanate from ACWI and NNRG). The results reveal not only a tripling of the causal links between the markets studied during the COVID-19 crisis period, but also a change in the causal structure between the two sub-periods, suggesting a *shift contagion* phenomenon during the COVID-19 crisis period — *i.e.*, the structure of causal links shifted during the COVID-19 crisis period relative to the pre-COVID-19 stress-free period. This *shift contagion* phenomenon is also observed, but to a lesser extent, during the ongoing Russian-Ukrainian conflict. Indeed, compared to the pre-war period, the period of the Russian-Ukrainian war is characterized by the presence of a relatively higher number of causal relationships between the markets considered. Indeed, we identify 21 causal relationships during the pre-war period and 26 during the war period (about 50% of which emanate from CLN and INV). Once again, this result suggests the existence of a *shift contagion* phenomenon during the ongoing war period, although to a lesser magnitude than that observed during the COVID-19 crisis period. During the pre-war period, BTCN and NRG have no impact on the other markets (see Table 5) and the other markets do not influence these two asset classes, which is why BTCN and NRG do not appear in Fig 2.c. This result shows that these two markets are totally isolated and not integrated with other markets during the pre-war period. Finally, the comparison of Figures 2.c and 2.d

reveals (i) a high increase in the number of causal links between INV and the other markets during the period of the Russian-Ukrainian war, and (ii) CLN has a greater impact during the war. This result shows that the war has raised investors interest in businesses engaged in the clean energy activities as well as businesses whose innovative technologies and services focus on generation and use of cleaner energy, conservation, efficiency and advancing renewable energy.

3.2. portfolio analysis

In this section we analyse two portfolio strategies composed of assets **ACWI**, **SBND**, **GRNB**, **IT**, **KLD**, **CLN**, **INV**, **BTCN**, **NRG** and **NNRG**. More specifically, we compare the minimum-causal-intensity (MIN-CAI) portfolio with the traditional Markowitz (1959) minimum-variance (MIN-VAR) portfolio. We are aware that an investor cannot directly buy an index. However, we make the implicit assumption that they can invest in a tracker or ETF that replicates the performance of the indexes under consideration.

Table 7 summarizes the portfolio weights during stress and stress-free periods under the two approaches – MIN-VAR and MIN-CAI. We find that the structure of the MIN-VAR portfolio differs clearly from that of the MIN-CAI portfolio. More interestingly, we find that the structure of the portfolios under the two approaches changed substantially once following the COVID-19 crisis and a second time following the onset of the Russian-Ukrainian conflict.

Table 7. Portfolio weights

	Pre-COV		COVID-19 period		Pre-War period		War period	
	MIN-VAR	MIN-CAI	MIN-VAR	MIN-CAI	MIN-VAR	MIN-CAI	MIN-VAR	MIN-CAI
ACWI	0.13	-0.05	0.54	0.09	0.10	-0.15	0.39	0.87
SBND	0.28	-0.04	0.45	-0.10	1.24	-0.03	1.88	-0.37
GRNB	0.52	0.20	0.12	0.05	-0.33	0.09	-1.22	-0.02
IT	-0.04	0.11	0.07	-0.15	-0.09	0.18	-0.03	0.69
KLD	0.05	0.13	-0.29	0.30	0.07	0.26	-0.08	0.54
CLN	0.01	0.09	0.03	0.01	0.02	0.31	-0.02	-0.19
INV	-0.04	0.16	-0.34	0.08	-0.05	-0.02	-0.03	-0.14
BTCN	0.00	0.14	-0.03	0.52	0.00	0.20	-0.02	0.44
NRG	0.00	0.22	0.00	0.05	0.00	0.20	-0.04	-0.16
NNRG	0.09	0.04	0.45	0.15	0.03	-0.04	0.17	-0.67
μ	0.05099	0.29980	-0.06289	-0.23658	-0.03213	1.30289	-0.13747	-0.39655
σ	0.00176	0.50775	0.00399	0.66908	0.00235	0.45017	0.00425	0.360511
SR	28.9737	0.5904	-15.7550	-0.3536	-13.6535	2.8942	-32.2943	-1.1000

Note: μ , σ and **SR** stand for “portfolio gross return”, “portfolio return standard-deviation” and “Sharpe ratio”, respectively. **MIN-VAR** and **MIN-CAI** stand for “minimum-variance portfolio” and “minimum-causal-intensity portfolio”, respectively. As in Tiwari et al. (2022), we compute the Sharpe ratio assuming that the risk-free rate is zero.

During the pre-COVID stress-free period, while the MIN-VAR method gives more weights to **GRNB**, **SBND** and **ACWI**, the MIN-CAI method give more weights to **NRG**, **GRNB** and **INV**. Portfolios compositions shifted significantly during the COVID-19 crisis period. Indeed, over this crisis period, the MIN-VAR portfolio method assigns the most important weights to **ACWI**, **SBND** and **NNRG**. During the same crisis period, the MIN-CAI method assigns the highest weights to **BTCN**, **KLD** and **NNRG**. The weights’ structure shifts again during the pre-war period. Indeed, during this period, the MIN-VAR portfolio method attributes the most important weights to **SBND**, while the MIN-CAI method favors **CLN**, **KLD**, **BTCN** and **NRG**. Over the Russian-Ukrainian war period, while the MIN-VAR method favors a “flight to quality” strategy

by giving more weight to **SBND**, the MIN-CAI method assigns more weight to **ACWI**, **IT**, **KLD** and **BTCN**.

During the pre-COVID and the pre-war periods, the portfolio analysis shows that the MIN-CAI portfolio outperforms the MIN-VAR portfolio in terms of gross return. Indeed, during these stress-free periods, the MIN-CAI method provides a portfolio structure characterized by a relatively higher return. However, this relatively high return-based performance is associated with a relatively higher level of risk, which is reflected in the relatively higher standard deviation of return. However, during the COVID-19 and war periods, the MIN-CAI portfolio not only results in a negative return (even more negative than that offered by the MIN-VAR portfolio), but it is also associated with relatively a higher level of risk.

Moreover, Table 7 reports the reward-to-volatility ratios (Sharpe, 1994), which divide the excess returns of portfolios by their respective volatilities to assess their risk-adjusted performances. In other words, the Sharpe ratio indicates the return that can be expected from a given portfolio with a risk equal to one standard deviation. The MIN-VAR portfolio records the highest reward-to-volatility ratio during the pre-COVID period, and the MIN-CAI outperforms during the pre-war period. Nevertheless, during both stress periods (the COVID-19 period and the Russian-Ukrainian war period), both methods result in negative Sharpe ratios.

4. Conclusion

Little attention has been paid in the literature to the impact of the COVID-19 crisis as well as the ongoing Russian-Ukrainian conflict on the causal links among financial markets. This paper fills this gap by (i) providing a quantitative assessment of the existence of *shift contagion* phenomena among a broad spectrum of financial markets (commodities, stocks, socially responsible investments, sovereign bonds, green bonds, cryptocurrencies, and clean energies) during recent stress periods (the COVID-19 crisis and the ongoing Russia-Ukraine war periods), and (ii) studying the implications for portfolio management. Thus, we first use TYDL causality test to investigate *shift contagion* and compute the causal intensities among the markets considered. Second, we use the results of the first step to propose a new portfolio method minimizing the causal intensity among the underlying assets.

The results of the TYDL causality test provide evidence of a structural change in the causal links between the financial markets under consideration during the two crisis periods examined. Indeed, the results show that the number of causal links between the markets considered almost tripled during the COVID-19 crisis period. More specifically, 20 causal links during the pre-COVID-19 period are identified, with a major influence of Bitcoin on the other markets, compared to 56 during the COVID-19 period. This finding reflects the existence of a strong *shift contagion* during the COVID-19 crisis. This *shift contagion* phenomenon is also observed during the ongoing Russia-Ukraine war period, although to a lesser extent than that observed during the COVID-19 crisis period. More interestingly, the Wilderhill Clean Energy Index (CLN) and the Wilderhill New Energy Global Innovation Index (INV) have the largest causal impact on the other financial markets during the war period. This result reflects the growing impact of companies engaged in clean energy activities as well as companies with innovative technologies on financial markets.

The portfolio analysis shows that the minimum-causal-intensity (MIN-CAI) portfolio method we propose suggests portfolio weights' structures that are different from those provided by the MIN-VAR method during both calm and turbulent periods. Moreover, the results show that the MIN-CAI portfolio outperforms the MIN-VAR portfolio in terms of gross return during the two stress-free periods examined. Nevertheless, this relatively outperformance in terms of return is associated with a relatively underperformance in terms of risk. During the COVID-19 crisis period and the Russian-Ukrainian war period, the proposed MIN-CAI portfolio method as well as the MIN-VAR benchmark method result in a negative return and higher levels of risk. Furthermore, the MIN-CAI portfolio records a lower reward-to-volatility ratio than the MIN-VAR portfolio during the pre-COVID period, and a higher ratio during the pre-war period. However, both portfolio approaches, the MIN-CAI approach and the MIN-VAR approach, record negative reward-to-volatility ratios during crisis periods.

References

- Aït-Sahalia, Y., Cacho-Diaz, J., & Laeven, R. J. (2015). Modeling financial contagion using mutually exciting jump processes. *Journal of Financial Economics*, 117(3), 585–606. <https://doi.org/10.1016/j.jfineco.2015.03.002>
- Arouri, M., Lahiani, A., & Nguyen, D. K. (2011). Return and volatility transmission between world oil prices and stock markets of the GCC countries. *Economic Modelling*, 28, 1815–1825. <https://doi.org/10.1016/j.econmod.2011.03.012>
- Asl, M. G., Canarella, G., & Miller, S. M. (2021). Dynamic asymmetric optimal portfolio allocation between energy stocks and energy commodities: Evidence from clean energy and oil and gas companies. *Resources Policy*, 71, 101982.
- Awartani, B., & Maghyereb, A. I. (2013). Dynamic spillovers between oil and stock markets in the Gulf Cooperation Council Countries. *Energy Economics*, 36, 28–42. <https://doi.org/10.1016/j.eneco.2012.11.024>
- Bala, D. A., & Takimoto T. (2017). Stock markets volatility spillovers during financial crises: A DCC-MGARCH with skewed-t density approach. *Borsa Istanbul Review*, 17(1), 25–48. <https://doi.org/10.1016/j.bir.2017.02.002>
- Barbaglia L., Croux, C., & Wilms, I. (2020). Volatility spillovers in commodity markets: A large t-vector autoregressive approach. *Energy Economics*, 85. <https://doi.org/10.1016/j.eneco.2019.104555>
- Basher, S. A., & Sadorsky, P. (2016). Hedging emerging market stock prices with oil, gold, VIX, and bonds: A comparison between DCC, ADCC and GO-GARCH. *Energy Economics*, 54, 235–247. <https://doi.org/10.1016/j.eneco.2015.11.022>
- Bélaïd, F., Ben Amar, A., Goutte, S., and Guesmi, K., (2021). Emerging and Advanced Economies Market Behavior During the COVID-19 Crisis Era, *International Journal of Finance and Economics*. DOI: <https://doi.org/10.1002/ijfe.2494>
- Belke, A., & Dubova, I. (2018). International spillovers in global asset markets. *Economic Systems*, 42(1), 3–17. <https://doi.org/10.1016/j.ecosys.2017.07.001>
- Ben Amar, A., Hachicha, N., & Halouani, N. (2020). Is there a shift contagion among stock markets during the COVID-19 crisis? Further insights from TYDL Causality Test. *International Review of Applied Economics*. <https://doi.org/10.1080/02692171.2020.1853685>
- Broadstock, D.C., Chan, K., Cheng, L.T.W., and Wang, X., (2021). The role of ESG performance during times of financial crisis: Evidence from COVID-19 in China, *Finance Research letters*, 38.
- Caporale, G. M., Pittis, N., & Spagnolo, N. (2002). Testing for causality-in-variance: An application to the east Asian markets. *International Journal of Finance and Economics*, 7, 235–245. <https://doi.org/10.1002/ijfe.185>
- Chang, C.-L., McAleer, M., & Tansuchat, R. (2011). Crude oil hedging strategies using dynamic multivariate GARCH. *Energy Economics*, 33, 912–923. <https://doi.org/10.1016/j.eneco.2011.01.009>

- Corbet, S., Hou, YG., Hu, Y., Larkin, C., Lucey, B., & Oxley, L., (2022). Cryptocurrency liquidity and volatility interrelationships during the COVID-19 pandemic, *Finance Research Letters*, 45.
- Corbet, S., Hou, YG., Hu, Y., Lucey, B., & Oxley, L., (2021). Aye Corona! The contagion effects of being named Corona during the COVID-19 pandemic, *Finance Research Letters*, 38.
- Corbet, S., Larkin, C., & Lucey, B., (2020). The contagion effects of the COVID-19 pandemic: Evidence from gold and cryptocurrencies, *Finance Research Letters*, 35.
- Diebold, F. X., & Yilmaz, K. (2009). Measuring financial asset return and volatility spillovers, with application to global equity markets. *Economic Journal*, 119(534), 158–171. <https://doi.org/10.1111/j.1468-0297.2008.02208.x>
- Dolado, J. J., & Lütkepohl, H. (1996). Making Wald Tests Work for Cointegrated VAR Systems, *Econometric Reviews*, 15(4), 369–386.
- Forbes, K. J., & Rigobon, R. (2002). No contagion, only interdependence: measuring stock market comovements. *Journal of Finance*, 57(5), 2223–2261. <https://doi.org/10.1111/0022-1082.00494>
- Gamba-Santamaria, S., Gomez-Gonzalez, J. E., Hurtado-Guarin, J. L., & Melo-Velandia, L. F. (2019). Volatility spillovers among global stock markets: Measuring total and directional effects. *Empirical Economics*, 56, 1581–1599. <https://doi.org/10.1007/s00181-017-1406-3>
- Ghorbel, A., Frikha, W., & Manzli, Y. S. (2022). Testing for asymmetric non-linear short-and long-run relationships between crypto-currencies and stock markets. *Eurasian Economic Review*, 1-39.
- Hemrit, W., & Benlagha, N. (2021). Does renewable energy index respond to the pandemic uncertainty?. *Renewable Energy*, 177, 336–347.
- Jeribi, A., & Masmoudi, W. K. (2021). Investigating dynamic interdependencies between traditional and digital assets during the COVID-19 outbreak: Implications for G7 and Chinese financial investors. *Journal of Research in Emerging Markets*, 3(3), 60–80.
- Kang, S. H., McIver, R., & Yoon, S-M. (2016). Modeling time-varying correlations in volatility between BRICS and commodity markets. *Emerging Markets Finance and Trade*, 52(7), 1698–1723. <https://doi:10.1080/1540496x.2016.1143248>
- Karolyi, G.A. (1995). A multivariate GARCH model of international transmissions of stock returns and volatility: The case of the United States and Canada. *Journal of Business and Economic Statistics*, 13(1), 11–25. <https://doi.org/10.2307/1392517>
- King, M. A., & Wadhvani, S. (1990). Transmission of volatility between stock markets. *Review of Financial Studies*, 3(1), 5–33.
- Kohlscheen, E., Mojon, B., and Rees D., The Macroeconomic Spillover Effects of the Pandemic on the Global Economy (April 6, 2020). BIS Bulletin no. 4., Available at SSRN: <https://ssrn.com/abstract=3569554> or <http://dx.doi.org/10.2139/ssrn.3569554>.

- Kwon, S., & Holliday, I. (2007). The Korean welfare state: A paradox of expansion in an era of globalisation and economic crisis. *International Journal of Social Welfare*, 16(3), 242–248. <https://doi.org/10.1111/j.1468-2397.2006.00457.x>
- Lee, J., Glenn, H., & Valera, A. (2015). Price transmission and volatility spillovers in Asian rice markets: Evidence from MGARCH and panel GARCH models. *The International Trade Journal*, 30(1), 1–20. <https://doi.org/10.1080/08853908.2015.1045638>
- Liu, S., Gao, H., Hou, P., & Tan, Y. (2019). Risk spillover effects of international crude oil market on China's major markets. *AIMS Energy*, 7(6), 819–840. <http://dx.doi.org/10.3934/energy.2019.6.819>
- Marais, E., & Bates, S. (2006). An Empirical Study to Identify Shift Contagion During the Asian crisis, *Journal of International Financial Markets, Institutions and Money*, 16(5), 468–479.
- Mieg, H.A. (2020). Volatility as a transmitter of systemic risk: Is there a structural risk in finance?. *Risk Analysis*. <https://doi.org/10.1111/risa.13564>
- Niu, H. (2021). Correlations between crude oil and stocks prices of renewable energy and technology companies: a multiscale time-dependent analysis. *Energy*, 221, 119800.
- Pan, Z., Wang, Y., Yang, L. (2014). Hedging crude oil using refined product: A regime switching asymmetric DCC approach. *Energy Economics*, 46, 472–484. <https://doi.org/10.1016/j.eneco.2014.05.014>
- Schwartz, H. (2012). Housing, the welfare state, and the global financial crisis: What is the connection?. *Politics & Society*, 40(1), 35–58. <https://doi.org/10.1177%2F0032329211434689>
- Sharpe, W. F. (1994). The Sharpe ratio. *Journal of Portfolio Management*, 21(1), 49–58.
- Silvennoinen, A., & Thorp, S. (2013). Financialization, crisis and commodity correlation dynamics. *Journal of International Financial Markets, Institutions and Money*, 24, 42–65. <https://doi.org/10.1016/j.intfin.2012.11.007>
- Tiwari, A. K., Abakah, E. J. A., Gabauer, D., & Dwumfour, R. A. (2022). Dynamic spillover effects among green bond, renewable energy stocks and carbon markets during COVID-19 pandemic: Implications for hedging and investments strategies. *Global Finance Journal*, 51, 100692.
- Toda, H. Y., & Yamamoto, T. (1995). Statistical Inference in Vector Autoregressions with Possibly Integrated Processes, *Journal of Econometrics*, 66(1-2), 225–250.
- Uddin, GS., Yahya, M., Goswami, GG., Lucey, B., & Ahmed, A., (2022). Stock market contagion during the COVID-19 pandemic in emerging economies, *International Review of Economics & Finance*, 79, 302-309
- Yarovaya, L., Brzeszczyński, J., Goodell, JW., Lucey, B., & Lau, CKM., (2022). Rethinking financial contagion: information transmission mechanism during the COVID-19 pandemic, *Journal of International Financial Markets, Institutions and Money*.

Zhang, D. & Broadstock, D. C. (2020). Global financial crisis and rising connectedness in the international commodity markets. *International Review of Financial Analysis*, 68(C). <https://doi.org/10.1016/j.irfa.2018.08.003>

Zhang, D., Hu, M., & Ji, Q. (2020). Financial markets under the global pandemic of COVID-19. *Finance Research Letters*, 36, 101528.

Appendices

Table 2. Descriptive statistics

Pre-COVID-19 period										
	ACWI	SBND	GRNB	IT	KLD	CLN	INV	BTCN	NRG	NNRG
Mean	6,25	4,71	4,63	5,59	6,99	4,08	5,25	8,83	5,29	5,79
Median	6,25	4,71	4,64	5,60	6,99	4,09	5,25	8,96	5,29	5,79
Max	6,34	4,74	4,66	5,76	7,10	4,26	5,40	9,44	5,43	5,83
Min	6,11	4,68	4,61	5,33	6,81	3,79	5,07	8,13	5,11	5,73
Std. Dev.	0,04	0,02	0,01	0,08	0,05	0,08	0,05	0,40	0,06	0,02
Skewness	-0,32	0,12	-0,13	-0,41	-0,46	-0,91	-0,02	-0,46	0,20	-0,60
Kurtosis	3,59	1,79	1,83	3,14	3,44	4,56	4,91	1,79	2,76	3,02
Jarque-Bera	8,20***	16,60***	15,79***	7,45***	11,24***	62,38***	39,75***	25,24***	2,40	15,44***
IO	1	1	1	1	1	1	1	1	0	0
COVID-19 period										
Mean	6,26	4,72	4,64	5,73	7,04	4,28	5,39	9,01	5,04	5,78
Median	6,34	4,71	4,64	5,78	7,10	4,34	5,45	9,07	5,15	5,79
Max	6,36	4,77	4,68	5,84	7,15	4,53	5,57	9,25	5,36	5,84
Min	5,95	4,69	4,57	5,47	6,74	3,86	5,05	8,52	4,40	5,66
Std. Dev.	0,13	0,02	0,02	0,11	0,12	0,17	0,14	0,18	0,30	0,05
Skewness	-1,15	1,40	-1,29	-1,08	-1,14	-1,07	-1,21	-0,93	-1,02	-0,81
Kurtosis	2,80	5,27	4,40	2,91	2,88	3,07	3,17	2,98	2,57	2,59
Jarque-Bera	14,42***	35,10***	23,34***	12,64***	14,04***	12,32***	15,86***	9,39***	11,81***	7,51**
IO	1	1	1	1	1	1	1	1	1	1
Pre-war period										
Mean	6,47	4,74	4,68	6,10	7,30	4,98	5,96	10,18	5,22	5,99
Median	6,52	4,74	4,69	6,15	7,32	5,09	6,08	10,50	5,32	6,04
Max	6,63	4,79	4,74	6,37	7,53	5,64	6,44	11,12	5,74	6,26
Min	6,05	4,66	4,59	5,56	6,84	3,93	5,15	8,76	4,16	5,66
Std. Dev.	0,14	0,03	0,03	0,19	0,17	0,38	0,30	0,73	0,34	0,16
Skewness	-0,81	-0,54	-0,75	-0,79	-0,48	-0,77	-0,87	-0,48	-0,60	-0,53
Kurtosis	2,54	2,95	2,72	2,79	2,20	2,96	2,88	1,61	2,70	1,95
Jarque-Bera	59,17***	24,25***	48,34***	52,37***	32,60***	48,93***	62,75***	58,93***	31,57***	45,78***
IO	1	1	1	1	1	1	1	1	1	1
War period										
Mean	6,44	4,54	4,46	6,08	7,33	4,70	5,81	10,19	5,86	6,22
Median	6,44	4,54	4,46	6,07	7,32	4,71	5,82	10,05	5,86	6,17
Max	6,58	4,67	4,61	6,27	7,48	4,96	5,99	10,77	6,06	6,36
Min	6,31	4,43	4,33	5,90	7,19	4,48	5,62	9,82	5,66	6,09
Std. Dev.	0,07	0,06	0,07	0,09	0,07	0,12	0,09	0,31	0,09	0,09
Skewness	0,11	0,06	0,00	0,12	0,11	0,08	-0,12	0,52	0,16	0,23
Kurtosis	2,11	2,31	2,18	2,12	2,11	2,00	1,97	1,66	2,29	1,33
Jarque-Bera	6,36**	3,79	5,18*	6,39**	6,45**	7,82**	8,61**	22,08**	4,57*	22,83***
IO	1	1	1	1	1	1	1	1	1	1

Note: Table 2 reports descriptive statistics of the log daily data. First row displays mean. second row displays median. Third and fourth rows show the largest and the smallest values, respectively. Fifth row displays standard deviation. Sixth and seventh rows skewness and kurtosis coefficients, respectively. Eighth row report Jarque-Bera normality test statistics. Ninth row displays the order of integration. As in Marais and Bates (2006) we use Phillips-Perron and KPSS tests to determine the order of integration.

Table 3. TYDL causality test results and causal intensities during the Pre-COVID-19 tranquil period

H1 hypothesis [X→Z]	I_{\max}	k	$p = k + I_{\max}$	Marginal significance levels of the TYDL	Decision	e_{zx}
ACWI→SBND	1	1	2	0.2821	Reject H1	ACWI↔SBND
ACWI→GRNB	1	1	2	0.4859	Reject H1	ACWI↔GRNB
ACWI→IT	1	1	2	0.0047	Accept H1	0.91
ACWI→KLD	1	2	3	0.0242	Accept H1	1.12
ACWI→CLN	1	1	2	0.7872	Reject H1	ACWI↔CLN
ACWI→INV	1	1	2	0.0117	Accept H1	0.84
ACWI→BTCN	1	1	2	0.9968	Reject H1	ACWI↔BTCN
ACWI→NRG	1	1	2	0.1601	Reject H1	ACWI↔NRG
ACWI→NNRG	1	1	2	0.6246	Reject H1	ACWI↔NNRG
SBND→ACWI	1	1	2	0.1939	Reject H1	SBND↔ACWI
SBND→GRNB	1	1	2	0.0016	Accept H1	0.98
SBND→IT	1	1	2	0.6997	Reject H1	SBND↔IT
SBND→KLD	1	1	2	0.2500	Reject H1	SBND↔KLD
SBND→CLN	1	1	2	0.3461	Reject H1	SBND↔CLN
SBND→INV	1	1	2	0.8179	Reject H1	SBND↔INV
SBND→BTCN	1	1	2	0.5321	Reject H1	SBND↔BTCN
SBND→NRG	1	1	2	0.7261	Reject H1	SBND↔NRG
SBND→NNRG	1	1	2	0.7225	Reject H1	SBND↔NNRG
GRNB→ACWI	1	1	2	0.1138	Reject H1	GRNB↔ACWI
GRNB→SBND	1	1	2	0.0034	Accept H1	1.01
GRNB→IT	1	1	2	0.1479	Reject H1	GRNB↔IT
GRNB→KLD	1	1	2	0.0986	Accept H1	1.51
GRNB→CLN	1	1	2	0.1055	Reject H1	GRNB↔CLN
GRNB→INV	1	1	2	0.6815	Reject H1	GRNB↔INV
GRNB→BTCN	1	1	2	0.2871	Reject H1	GRNB↔BTCN
GRNB→NRG	1	1	2	0.5177	Reject H1	GRNB↔NRG
GRNB→NNRG	1	1	2	0.7545	Reject H1	GRNB↔NNRG
IT→ACWI	1	1	2	0.0027	Accept H1	1.10
IT→SBND	1	1	2	0.8486	Reject H1	IT↔SBND
IT→GRNB	1	1	2	0.8348	Reject H1	IT↔GRNB
IT→KLD	1	1	2	0.1493	Reject H1	IT↔KLD
IT→CLN	1	1	2	0.0996	Accept H1	0.73
IT→INV	1	1	2	0.8703	Reject H1	IT↔INV
IT→BTCN	1	1	2	0.7797	Reject H1	IT↔BTCN
IT→NRG	1	1	2	0.9715	Reject H1	IT↔NRG
IT→NNRG	1	1	2	0.2029	Reject H1	IT↔NNRG
KLD→ACWI	1	2	3	0.0408	Accept H1	0.89
KLD→SBND	1	1	2	0.8508	Reject H1	KLD↔SBND
KLD→GRNB	1	1	2	0.9021	Reject H1	KLD↔GRNB
KLD→IT	1	1	2	0.2015	Reject H1	KLD↔IT
KLD→CLN	1	1	2	0.0996	Accept H1	0.59
KLD→INV	1	2	3	0.1458	Reject H1	KLD↔INV
KLD→BTCN	1	1	2	0.7927	Reject H1	KLD↔BTCN
KLD→NRG	1	1	2	0.3692	Reject H1	KLD↔NRG
KLD→NNRG	1	1	2	0.2638	Reject H1	KLD↔NNRG
CLN→ACWI	1	1	2	0.2593	Reject H1	CLN↔ACWI
CLN→SBND	1	1	2	0.9235	Reject H1	CLN↔SBND
CLN→GRNB	1	1	2	0.8177	Reject H1	CLN↔GRNB
CLN→IT	1	1	2	0.0632	Accept H1	1.35
CLN→KLD	1	1	2	0.1384	Reject H1	CLN↔KLD
CLN→INV	1	2	3	0.1427	Reject H1	CLN↔INV
CLN→BTCN	1	1	2	0.9988	Reject H1	CLN↔BTCN
CLN→NRG	1	1	2	0.5088	Reject H1	CLN↔NRG
CLN→NNRG	1	1	2	0.1667	Reject H1	CLN↔NNRG
INV→ACWI	1	1	2	0.5324	Reject H1	INV↔ACWI
INV→SBND	1	1	2	0.3963	Reject H1	INV↔SBND
INV→GRNB	1	1	2	0.5579	Reject H1	INV↔GRNB
INV→IT	1	1	2	0.0369	Accept H1	1.07
INV→KLD	1	2	3	0.1086	Reject H1	INV↔KLD
INV→CLN	1	2	3	0.4619	Reject H1	INV↔CLN
INV→BTCN	1	1	2	0.8036	Reject H1	INV↔BTCN
INV→NRG	1	1	2	0.1056	Reject H1	INV↔NRG
INV→NNRG	1	1	2	0.5084	Reject H1	INV↔NNRG
BTCN→ACWI	1	1	2	0.3144	Reject H1	BTCN↔ACWI
BTCN→SBND	1	1	2	0.3046	Reject H1	BTCN↔SBND
BTCN→GRNB	1	1	2	0.8605	Reject H1	BTCN↔GRNB

BTCN→IT	1	1	2	0.4137	Reject H1	BTCN→IT
BTCN→KLD	1	1	2	0.7011	Reject H1	BTCN→KLD
BTCN→CLN	1	1	2	0.0649	Accept H1	0.31
BTCN→INV	1	1	2	0.0259	Accept H1	0.54
BTCN→NRG	1	1	2	0.0176	Accept H1	0.56
BTCN→NNRG	1	1	2	0.0181	Accept H1	-0.15
NRG→ACWI	1	1	2	0.5568	Reject H1	NRG→ACWI
NRG→SBND	1	1	2	0.0786	Accept H1	0.91
NRG→GRNB	1	1	2	0.2559	Reject H1	NRG→GRNB
NRG→IT	1	1	2	0.5139	Reject H1	NRG→IT
NRG→KLD	1	1	2	0.8614	Reject H1	NRG→KLD
NRG→CLN	1	1	2	0.8939	Reject H1	NRG→CLN
NRG→INV	1	1	2	0.6413	Reject H1	NRG→INV
NRG→BTCN	1	1	2	0.7912	Reject H1	NRG→BTCN
NRG→NNRG	0	1	1	0.1523	Reject H1	NRG→NNRG
NNRG→ACWI	1	1	2	0.1593	Reject H1	NNRG→ACWI
NNRG→SBND	1	1	2	0.6749	Reject H1	NNRG→SBND
NNRG→GRNB	1	1	2	0.5908	Reject H1	NNRG→GRNB
NNRG→IT	1	1	2	0.0657	Accept H1	0.98
NNRG→KLD	1	1	2	0.1088	Reject H1	NNRG→KLD
NNRG→CLN	1	1	2	0.4225	Reject H1	NNRG→CLN
NNRG→INV	1	1	2	0.0345	Accept H1	0.91
NNRG→BTCN	1	1	2	0.7525	Reject H1	NNRG→BTCN
NNRG→NRG	0	1	1	0.0002	Accept H1	0.92

Note: To take into account the highest number of potential causal links while minimizing the risk of imprecision, a 10% significance level was used for all causality tests.

Table 4. TYDL causality test results and causal intensities during the COVID-19 crisis period (Quarter 1, 2020)

H1 hypothesis [X→Z]	I _{max}	k	p = k + I _{max}	Marginal significance levels of the TYDL	Decision	e _{ZX}
ACWI→SBND	1	3	4	0.0004	Accept H1	0.80
ACWI→GRNB	1	7	8	0.0000	Accept H1	0.73
ACWI→IT	1	2	3	0.0438	Accept H1	0.91
ACWI→KLD	1	2	3	0.0099	Accept H1	1.15
ACWI→CLN	1	1	2	0.0004	Accept H1	0.67
ACWI→INV	1	2	3	0.0458	Accept H1	0.86
ACWI→BTCN	1	1	2	0.9670	Reject H1	ACWI↔BTCN
ACWI→NRG	1	4	5	0.0213	Accept H1	0.90
ACWI→NNRG	1	2	3	0.0051	Accept H1	1.05
SBND→ACWI	1	3	4	0.0018	Accept H1	1.27
SBND→GRNB	1	3	4	0.4308	Reject H1	SBND↔GRNB
SBND→IT	1	3	4	0.0002	Accept H1	1.19
SBND→KLD	1	3	4	0.0004	Accept H1	1.45
SBND→CLN	1	2	3	0.1077	Reject H1	SBND↔CLN
SBND→INV	1	2	3	0.1626	Reject H1	SBND↔INV
SBND→BTCN	1	1	2	0.9490	Reject H1	SBND↔BTCN
SBND→NRG	1	2	3	0.6125	Reject H1	SBND↔NRG
SBND→NNRG	1	2	3	0.3469	Reject H1	SBND↔NNRG
GRNB→ACWI	1	7	8	0.0000	Accept H1	1.37
GRNB→SBND	1	3	4	0.0004	Accept H1	1.01
GRNB→IT	1	5	6	0.0000	Accept H1	1.26
GRNB→KLD	1	5	6	0.0000	Accept H1	1.54
GRNB→CLN	1	3	4	0.0024	Accept H1	0.88
GRNB→INV	1	2	3	0.0650	Accept H1	1.15
GRNB→BTCN	1	2	3	0.4350	Reject H1	GRNB↔BTCN
GRNB→NRG	1	2	3	0.1361	Reject H1	GRNB↔NRG
GRNB→NNRG	1	2	3	0.5393	Reject H1	GRNB↔NNRG
IT→ACWI	1	2	3	0.1890	Reject H1	IT↔ACWI
IT→SBND	1	3	4	0.0004	Accept H1	0.84
IT→GRNB	1	5	6	0.0040	Accept H1	0.80
IT→KLD	1	2	3	0.0956	Accept H1	1.22
IT→CLN	1	2	3	0.0106	Accept H1	0.74
IT→INV	1	2	3	0.5258	Reject H1	IT↔INV
IT→BTCN	1	2	3	0.2525	Reject H1	IT↔BTCN
IT→NRG	1	4	5	0.0108	Accept H1	0.99
IT→NNRG	1	2	3	0.0501	Accept H1	1.04
KLD→ACWI	1	2	3	0.1249	Reject H1	KLD↔ACWI
KLD→SBND	1	3	4	0.0007	Accept H1	0.68
KLD→GRNB	1	5	6	0.0085	Accept H1	0.65
KLD→IT	1	2	3	0.1116	Reject H1	KLD↔IT
KLD→CLN	1	2	3	0.0075	Accept H1	0.60
KLD→INV	1	2	3	0.3451	Reject H1	KLD↔INV
KLD→BTCN	1	2	3	0.2781	Reject H1	KLD↔BTCN
KLD→NRG	1	4	5	0.0042	Accept H1	0.80
KLD→NNRG	1	2	3	0.0185	Accept H1	0.36
CLN→ACWI	1	1	2	0.0056	Accept H1	1.49
CLN→SBND	1	2	3	0.0001	Accept H1	1.14
CLN→GRNB	1	3	4	0.0014	Accept H1	1.07
CLN→IT	1	2	3	0.0579	Accept H1	1.34
CLN→KLD	1	2	3	0.0835	Accept H1	1.66
CLN→INV	1	3	4	0.2325	Reject H1	CLN↔INV
CLN→BTCN	1	1	2	0.8965	Reject H1	CLN↔BTCN
CLN→NRG	1	1	2	0.6802	Reject H1	CLN↔NRG
CLN→NNRG	1	1	2	0.0072	Accept H1	1.41
INV→ACWI	1	2	3	0.0114	Accept H1	1.17
INV→SBND	1	2	3	0.0006	Accept H1	0.90
INV→GRNB	1	2	3	0.0045	Accept H1	0.85
INV→IT	1	2	3	0.0413	Accept H1	1.06
INV→KLD	1	2	3	0.0090	Accept H1	1.31
INV→CLN	1	3	4	0.1163	Reject H1	INV↔CLN
INV→BTCN	1	1	2	0.6828	Reject H1	INV↔BTCN
INV→NRG	1	1	2	0.9566	Reject H1	INV↔NRG
INV→NNRG	1	1	2	0.0689	Accept H1	1.11
BTCN→ACWI	1	1	2	0.7735	Reject H1	BTCN↔ACWI
BTCN→SBND	1	1	2	0.0036	Accept H1	0.52

BTCN→GRNB	1	2	3	0.2698	Reject H1	BTCN↔GRNB
BTCN→IT	1	2	3	0.0922	Accept H1	0.62
BTCN→KLD	1	2	3	0.1136	Reject H1	BTCN↔KLD
BTCN→CLN	1	1	2	0.9490	Reject H1	BTCN↔CLN
BTCN→INV	1	1	2	0.7427	Reject H1	BTCN↔INV
BTCN→NRG	1	1	2	0.3019	Reject H1	BTCN↔NRG
BTCN→NNRG	1	1	2	0.9759	Reject H1	BTCN↔NNRG
NRG→ACWI	1	4	5	0.0001	Accept H1	1.24
NRG→SBND	1	2	3	0.0002	Accept H1	0.74
NRG→GRNB	1	2	3	0.0053	Accept H1	1.02
NRG→IT	1	4	5	0.0009	Accept H1	1.19
NRG→KLD	1	4	5	0.0001	Accept H1	1.40
NRG→CLN	1	1	2	0.6675	Reject H1	NRG↔CLN
NRG→INV	1	1	2	0.4179	Reject H1	NRG↔INV
NRG→BTCN	1	1	2	0.2365	Reject H1	NRG↔BTCN
NRG→NNRG	1	2	3	0.0189	Accept H1	1.01
NNRG→ACWI	1	2	3	0.0060	Accept H1	1.07
NNRG→SBND	1	2	3	0.0210	Accept H1	0.82
NNRG→GRNB	1	2	3	0.0233	Accept H1	0.80
NNRG→IT	1	2	3	0.0149	Accept H1	0.99
NNRG→KLD	1	2	3	0.0558	Accept H1	1.21
NNRG→CLN	1	1	2	0.0009	Accept H1	0.74
NNRG→INV	1	1	2	0.0022	Accept H1	0.93
NNRG→BTCN	1	1	2	0.6954	Reject H1	NNRG↔BTCN
NNRG→NRG	1	2	3	0.0372	Accept H1	0.97

Note: To take into account the highest number of potential causal links while minimizing the risk of imprecision, a 10% significance level was used for all causality tests.

Table 5. TYDL causality test results and causal intensities during the Pre-Ukrainian-war period

H1 hypothesis [X→Z]	I_{\max}	k	$p = k + I_{\max}$	Marginal significance levels of the TYDL	Decision	e_{zx}
ACWI→SBND	1	1	2	0.0000	Accept H1	0.75
ACWI→GRNB	1	2	3	0.0000	Accept H1	0.72
ACWI→IT	1	1	2	0.1248	Reject H1	ACWI→IT
ACWI→KLD	1	2	3	0.3303	Reject H1	ACWI→KLD
ACWI→CLN	1	1	2	0.1459	Reject H1	ACWI→CLN
ACWI→INV	1	1	2	0.8009	Reject H1	ACWI→INV
ACWI→BTCN	1	1	2	0.1615	Reject H1	ACWI→BTCN
ACWI→NRG	1	1	2	0.2668	Reject H1	ACWI→NRG
ACWI→NNRG	1	1	2	0.0554	Accept H1	0.95
SBND→ACWI	1	1	2	0.1966	Reject H1	SBND→ACWI
SBND→GRNB	1	1	2	0.5580	Reject H1	SBND→GRNB
SBND→IT	1	1	2	0.8318	Reject H1	SBND→IT
SBND→KLD	1	2	3	0.2376	Reject H1	SBND→KLD
SBND→CLN	1	1	2	0.3132	Reject H1	SBND→CLN
SBND→INV	1	2	3	0.0578	Accept H1	1.27
SBND→BTCN	1	1	2	0.2737	Reject H1	SBND→BTCN
SBND→NRG	1	1	2	0.3630	Reject H1	SBND→NRG
SBND→NNRG	1	1	2	0.2993	Reject H1	SBND→NNRG
GRNB→ACWI	1	2	3	0.0246	Accept H1	1.39
GRNB→SBND	1	1	2	0.6283	Reject H1	GRNB→SBND
GRNB→IT	1	2	3	0.4409	Reject H1	GRNB→IT
GRNB→KLD	1	2	3	0.1996	Reject H1	GRNB→KLD
GRNB→CLN	1	2	3	0.1287	Reject H1	GRNB→CLN
GRNB→INV	1	2	3	0.0071	Accept H1	1.29
GRNB→BTCN	1	1	2	0.2148	Reject H1	GRNB→BTCN
GRNB→NRG	1	1	2	0.2578	Reject H1	GRNB→NRG
GRNB→NNRG	1	1	2	0.2676	Reject H1	GRNB→NNRG
IT→ACWI	1	1	2	0.7151	Reject H1	IT→ACWI
IT→SBND	1	1	2	0.0001	Accept H1	0.79
IT→GRNB	1	2	3	0.0000	Accept H1	0.76
IT→KLD	1	1	2	0.5422	Reject H1	IT→KLD
IT→CLN	1	1	2	0.1772	Reject H1	IT→CLN
IT→INV	1	1	2	0.4941	Reject H1	IT→INV
IT→BTCN	1	1	2	0.2899	Reject H1	IT→BTCN
IT→NRG	1	1	2	0.1567	Reject H1	IT→NRG
IT→NNRG	1	1	2	0.1109	Reject H1	IT→NNRG
KLD→ACWI	1	2	3	0.0213	Accept H1	0.83
KLD→SBND	1	2	3	0.0001	Accept H1	0.66
KLD→GRNB	1	2	3	0.0000	Accept H1	0.64
KLD→IT	1	1	2	0.3090	Reject H1	KLD→IT
KLD→CLN	1	1	2	0.2744	Reject H1	KLD→CLN
KLD→INV	1	2	3	0.4064	Reject H1	KLD→INV
KLD→BTCN	1	1	2	0.3603	Reject H1	KLD→BTCN
KLD→NRG	1	1	2	0.4074	Reject H1	KLD→NRG
KLD→NNRG	1	1	2	0.0219	Accept H1	0.84
CLN→ACWI	1	1	2	0.0325	Accept H1	1.17
CLN→SBND	1	1	2	0.0009	Accept H1	1.01
CLN→GRNB	1	2	3	0.0000	Accept H1	0.94
CLN→IT	1	1	2	0.1025	Reject H1	CLN→IT
CLN→KLD	1	1	2	0.2044	Reject H1	CLN→KLD
CLN→INV	1	2	3	0.0090	Accept H1	1.18
CLN→BTCN	1	1	2	0.9412	Reject H1	CLN→BTCN
CLN→NRG	1	1	2	0.6575	Reject H1	CLN→NRG
CLN→NNRG	1	1	2	0.0416	Accept H1	0.57
INV→ACWI	1	1	2	0.2218	Reject H1	INV→ACWI
INV→SBND	1	2	3	0.0022	Accept H1	0.82
INV→GRNB	1	2	3	0.0000	Accept H1	0.78
INV→IT	1	1	2	0.1843	Reject H1	INV→IT
INV→KLD	1	2	3	0.2598	Reject H1	INV→KLD
INV→CLN	1	2	3	0.1850	Reject H1	INV→CLN
INV→BTCN	1	1	2	0.5265	Reject H1	INV→BTCN
INV→NRG	1	1	2	0.6738	Reject H1	INV→NRG
INV→NNRG	1	1	2	0.2094	Reject H1	INV→NNRG
BTCN→ACWI	1	1	2	0.5884	Reject H1	BTCN→ACWI
BTCN→SBND	1	1	2	0.2567	Reject H1	BTCN→SBND
BTCN→GRNB	1	1	2	0.1092	Reject H1	BTCN→GRNB

BTCN→IT	1	1	2	0.8631	Reject H1	BTCN↔IT
BTCN→KLD	1	1	2	0.7440	Reject H1	BTCN↔KLD
BTCN→CLN	1	1	2	0.2479	Reject H1	BTCN↔CLN
BTCN→INV	1	1	2	0.1837	Reject H1	BTCN↔INV
BTCN→NRG	1	1	2	0.1980	Reject H1	BTCN↔NRG
BTCN→NNRG	1	1	2	0.6824	Reject H1	BTCN↔NNRG
NRG→ACWI	1	1	2	0.3332	Reject H1	NRG↔ACWI
NRG→SBND	1	1	2	0.7330	Reject H1	NRG↔SBND
NRG→GRNB	1	1	2	0.1790	Reject H1	NRG↔GRNB
NRG→IT	1	1	2	0.4387	Reject H1	NRG↔IT
NRG→KLD	1	1	2	0.5426	Reject H1	NRG↔KLD
NRG→CLN	1	1	2	0.1660	Reject H1	NRG↔CLN
NRG→INV	1	1	2	0.1904	Reject H1	NRG↔INV
NRG→BTCN	1	1	2	0.4647	Reject H1	NRG↔BTCN
NRG→NNRG	1	1	2	0.5529	Reject H1	NRG↔NNRG
NNRG→ACWI	1	1	2	0.2257	Reject H1	NNRG↔ACWI
NNRG→SBND	1	1	2	0.7827	Reject H1	NNRG↔SBND
NNRG→GRNB	1	1	2	0.7471	Reject H1	NNRG↔GRNB
NNRG→IT	1	1	2	0.1739	Reject H1	NNRG↔IT
NNRG→KLD	1	1	2	0.2426	Reject H1	NNRG↔KLD
NNRG→CLN	1	1	2	0.0225	Accept H1	0.86
NNRG→INV	1	1	2	0.0344	Accept H1	1.04
NNRG→BTCN	1	1	2	0.4864	Reject H1	NNRG↔BTCN
NNRG→NRG	1	1	2	0.9139	Reject H1	NNRG↔NRG

Note: To take into account the highest number of potential causal links while minimizing the risk of imprecision, a 10% significance level was used for all causality tests.

Table 6. TYDL causality test results and causal intensities during the Russia-Ukraine war period

H1 hypothesis [X→Z]	I_{max}	k	$p = k + I_{max}$	Marginal significance levels of the TYDL	Decision	e_{zx}
ACWI→SBND	1	1	2	0.0038	Accept H1	0.72
ACWI→GRNB	1	1	2	0.0014	Accept H1	0.40
ACWI→IT	1	2	3	0.5154	Reject H1	ACWI→IT
ACWI→KLD	1	2	3	0.6952	Reject H1	ACWI→KLD
ACWI→CLN	1	1	2	0.5942	Reject H1	ACWI→CLN
ACWI→INV	1	1	2	0.7660	Reject H1	ACWI→INV
ACWI→BTCN	1	1	2	0.7602	Reject H1	ACWI→BTCN
ACWI→NRG	1	1	2	0.0596	Accept H1	0.91
ACWI→NNRG	1	1	2	0.0108	Accept H1	0.96
SBND→ACWI	1	1	2	0.6789	Reject H1	SBND→ACWI
SBND→GRNB	1	1	2	0.2766	Reject H1	SBND→GRNB
SBND→IT	1	1	2	0.8180	Reject H1	SBND→IT
SBND→KLD	1	1	2	0.5689	Reject H1	SBND→KLD
SBND→CLN	1	1	2	0.8133	Reject H1	SBND→CLN
SBND→INV	1	1	2	0.7191	Reject H1	SBND→INV
SBND→BTCN	1	1	2	0.2409	Reject H1	SBND→BTCN
SBND→NRG	1	1	2	0.0198	Accept H1	1.29
SBND→NNRG	1	1	2	0.7394	Reject H1	SBND→NNRG
GRNB→ACWI	1	1	2	0.3730	Reject H1	GRNB→ACWI
GRNB→SBND	1	1	2	0.0848	Accept H1	1.02
GRNB→IT	1	1	2	0.4023	Reject H1	GRNB→IT
GRNB→KLD	1	1	2	0.2875	Reject H1	GRNB→KLD
GRNB→CLN	1	1	2	0.5449	Reject H1	GRNB→CLN
GRNB→INV	1	1	2	0.4032	Reject H1	GRNB→INV
GRNB→BTCN	1	1	2	0.2184	Reject H1	GRNB→BTCN
GRNB→NRG	1	1	2	0.0266	Accept H1	1.31
GRNB→NNRG	1	1	2	0.7315	Reject H1	GRNB→NNRG
IT→ACWI	1	2	3	0.7824	Reject H1	IT→ACWI
IT→SBND	1	1	2	0.0159	Accept H1	0.75
IT→GRNB	1	1	2	0.0063	Accept H1	0.74
IT→KLD	1	1	2	0.8531	Reject H1	IT→KLD
IT→CLN	1	1	2	0.4536	Reject H1	IT→CLN
IT→INV	1	1	2	0.5712	Reject H1	IT→INV
IT→BTCN	1	1	2	0.9554	Reject H1	IT→BTCN
IT→NRG	1	1	2	0.0671	Accept H1	0.96
IT→NNRG	1	1	2	0.0235	Accept H1	1.02
KLD→ACWI	1	2	3	0.5752	Reject H1	KLD→ACWI
KLD→SBND	1	1	2	0.0025	Accept H1	0.69
KLD→GRNB	1	1	2	0.0006	Accept H1	0.57
KLD→IT	1	1	2	0.8801	Reject H1	KLD→IT
KLD→CLN	1	1	2	0.3388	Reject H1	KLD→CLN
KLD→INV	1	1	2	0.6849	Reject H1	KLD→INV
KLD→BTCN	1	1	2	0.7395	Reject H1	KLD→BTCN
KLD→NRG	1	1	2	0.1736	Reject H1	KLD→NRG
KLD→NNRG	1	1	2	0.0214	Accept H1	0.84
CLN→ACWI	1	1	2	0.0908	Accept H1	1.38
CLN→SBND	1	1	2	0.0938	Accept H1	0.98
CLN→GRNB	1	1	2	0.0453	Accept H1	0.96
CLN→IT	1	1	2	0.1957	Reject H1	CLN→IT
CLN→KLD	1	1	2	0.1824	Reject H1	CLN→KLD
CLN→INV	1	2	3	0.6656	Reject H1	CLN→INV
CLN→BTCN	1	1	2	0.0811	Accept H1	2.01
CLN→NRG	1	1	2	0.0115	Accept H1	1.25
CLN→NNRG	1	1	2	0.0310	Accept H1	1.30
INV→ACWI	1	1	2	0.0906	Accept H1	1.11
INV→SBND	1	1	2	0.0614	Accept H1	0.79
INV→GRNB	1	1	2	0.0332	Accept H1	0.78
INV→IT	1	1	2	0.2225	Reject H1	INV→IT
INV→KLD	1	1	2	0.1747	Reject H1	INV→KLD
INV→CLN	1	2	3	0.7712	Reject H1	INV→CLN
INV→BTCN	1	1	2	0.0128	Accept H1	1.69
INV→NRG	1	1	2	0.0099	Accept H1	1.01
INV→NNRG	1	1	2	0.0184	Accept H1	1.06
BTCN→ACWI	1	1	2	0.7849	Reject H1	BTCN→ACWI
BTCN→SBND	1	1	2	0.7287	Reject H1	BTCN→SBND
BTCN→GRNB	1	1	2	0.4320	Reject H1	BTCN→GRNB

BTCN→IT	1	1	2	0.8224	Reject H1	BTCN↔IT
BTCN→KLD	1	1	2	0.6462	Reject H1	BTCN↔KLD
BTCN→CLN	1	1	2	0.5723	Reject H1	BTCN↔CLN
BTCN→INV	1	1	2	0.3837	Reject H1	BTCN↔INV
BTCN→NRG	1	1	2	0.3282	Reject H1	BTCN↔NRG
BTCN→NNRG	1	1	2	0.2736	Reject H1	BTCN↔NNRG
NRG→ACWI	1	1	2	0.5967	Reject H1	NRG↔ACWI
NRG→SBND	1	1	2	0.2100	Reject H1	NRG↔SBND
NRG→GRNB	1	1	2	0.2135	Reject H1	NRG↔GRNB
NRG→IT	1	1	2	0.9248	Reject H1	NRG↔IT
NRG→KLD	1	1	2	0.8256	Reject H1	NRG↔KLD
NRG→CLN	1	1	2	0.5482	Reject H1	NRG↔CLN
NRG→INV	1	1	2	0.8321	Reject H1	NRG↔INV
NRG→BTCN	1	1	2	0.6792	Reject H1	NRG↔BTCN
NRG→NNRG	1	1	2	0.3509	Reject H1	NRG↔NNRG
NNRG→ACWI	1	1	2	0.6559	Reject H1	NNRG↔ACWI
NNRG→SBND	1	1	2	0.3422	Reject H1	NNRG↔SBND
NNRG→GRNB	1	1	2	0.4079	Reject H1	NNRG↔GRNB
NNRG→IT	1	1	2	0.8375	Reject H1	NNRG↔IT
NNRG→KLD	1	1	2	0.8979	Reject H1	NNRG↔KLD
NNRG→CLN	1	1	2	0.4884	Reject H1	NNRG↔CLN
NNRG→INV	1	1	2	0.9148	Reject H1	NNRG↔INV
NNRG→BTCN	1	1	2	0.4947	Reject H1	NNRG↔BTCN
NNRG→NRG	1	1	2	0.7192	Reject H1	NNRG↔NRG

Note: To take into account the highest number of potential causal links while minimizing the risk of imprecision, a 10% significance level was used for all causality tests.